ICG-001, A Novel Small Molecule Regulator of TCF/β-Catenin Transcription

Masakatsu Eguchi[a], Cu Nguyen[a], Sung Chan Lee[a] and Michael Kahn[a,b,*]

[a]*Institute for Chemical Genomics, 600 Broadway, Suite 580, Seattle, WA 98122, USA and* [b]*Department of Pathobiology, University of Washington, Seattle, WA 98195, USA*

Abstract: Inherited and somatic mutations in the APC gene, a human tumor-suppressor, occur in a large percentage of colon cancers, leading to elevated levels of nuclear β-Catenin, and to activation of TCF/β-Catenin-responsive genes including cyclin D1 and c-myc. To identify small molecule antagonists of this pathway, we screened transformed colorectal cells with a secondary structure-templated chemical library, in search of compounds that attenuated a TCF/β-Catenin-responsive reporter gene. From this library we selected ICG-001 (IC_{50} = 3 μM) as a lead compound. Design and synthesis of the chemical library and some preliminary biological evaluation is described.

Key Words: Peptidomimetics, Anti-cancer, Wnt Pathway, β-Catenin.

INTRODUCTION

The Wnt/β-catenin pathway initiates a signaling cascade that is critical in balancing cell proliferation versus cell differentiation in normal tissue growth and the development of cancer under pathogenic circumstances [1-4]. The hallmark of this pathway is that it activates the transcriptional role of the multifunctional protein β-catenin, which is found in the cytoplasm and nucleus where it regulates transcription [5]. β-Catenin is regulated *via* phosphorylation by glycogen synthase kinase-3β (GSK-3β), casein kinase-1α (CK-1α), the scaffold protein, Axin, and the tumor suppressor, adenomatous polyposis coli (APC), among others [6]. In the absence of Wnt signaling, phosphorylation of β-catenin constantly takes place followed by Skp1-Cullin-F box (SCF)-directed ubiquitination, which results in proteosomal degradation of the β-catenin. Canonical Wnt signaling inactivates GSK-3β, preventing β-catenin phosphorylation. This leads to accumulation of β-catenin in the cytoplasm and subsequent translocation to the nucleus. A key step in the activation of target genes is the formation of a complex between β-catenin and members of the T-cell factor (TCF)/ lymphoid enhancer factor (LEF-1) family of transcription factors in nucleus [7]. To generate a transcriptionally active complex, β-catenin recruits the transcriptional coactivators, Creb-Binding Protein (CBP) or its closely related homolog, p300 [8,9] as well as other components of the basal transcription machinery.

The Wnt/β-catenin pathway normally regulates the expression of a range of genes involved in promoting proliferation and differentiation. Misregulation of this pathway is associated with a range of diseases [10]. In more than 85% of colon cancers, one of the components of the destruction complex, APC and/or β-catenin itself, is mutated, leading to an increase in nuclear β-catenin and constitutive expression of target genes [11]. Many of these genes, including *cyclin D1* [12,13] and *c-myc* [14], which play critical roles in cell growth, proliferation, and differentiation are inappropriately activated in colon cancer. Given that the majority of colorectal cancers involve activation of the β-catenin signaling pathway, and given the fact that multiple mutations lead to this activation, there is a clear need for drugs that attenuate the nuclear functions of β-catenin [15].

We have developed a β-turn peptidomimetic template with four sites of diversity readily accessible through solid phase synthesis from commercially available diversity components [16,17]. β-Turns constitute tetrapeptide units that cause a reversal of direction of the peptide chain. Formally, turns can be described by the distance from the Cα of the first residue to the Cα of the fourth residue (Fig. (**1**a)). When this distance is less than 7 Å and the tetrapeptide sequence is not in an α-helical region, it is considered a β-turn. β-Turns are classified according to the φ and ψ angles of the i + 1 and i + 2 residues. In addition to a number of turn types (I, I', II, II', III, III', IV, V, Va, VIa, VIb, VII, and VIII), the Cα(i) to Cα(i+3) distance varies from 4 ~ 7 Å [18]. A 6,6-bicyclic structure was chosen to mimic one of these β-turn structures, which afford proper placements of the functional groups to mimic the i + 1 and i +2 side chains of β-turn and accommodation of the incoming and outgoing peptide chains (e.g., i and i +3 functionalities) (Fig. (**1**b)). Our Monte Carlo conformational analysis of the bicyclic templates, **6** and **8**, using the MMFF force field *in vacuo* as

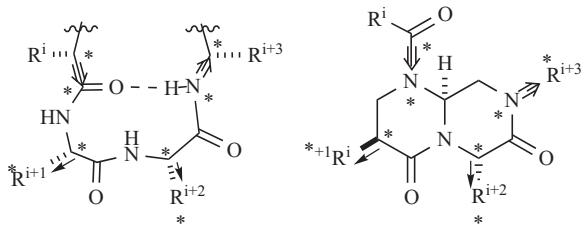

Fig. (1). The structure of β-turn and bicyclic β-turn mimetics.

*Address correspondence to this author at the Institute for Chemical Genomics, 600 Broadway, Suite 580, Seattle, WA 98122, USA; E-mail: mkahn@ichemgen.org

1573-4064/05 $50.00+.00

implemented in MacroModel, revealed a dominant pseudo-axial orientation of the R_{i+2} for low energy conformers. All conformations with a Boltzmann population of more than 0.5% were compared with idealized β-turns (type I, I', II, II', VIa and VIb) [18] at seven positions. Good RMSD values (0.38-0.50Å) were obtained for a type I β-turn conformation. Furthermore, this privileged template was shown by X-ray crystal structural analysis and solution phase 2D-NMR spectroscopy to mimic a type I β−turn conformation accurately on a rigid bicyclic structure [16].

Secondary structure elements, such as β-turns, β-strands, and α-helices, in proteins play key roles in molecular recognition events in biological systems through their characteristic three-dimensional presentation of functional groups. In addition, the conformationally constrained peptidomimetics pay a lower entropy cost upon binding to their target protein. Therefore, libraries of secondary structure mimetics may have a significantly higher success ratio in disrupting protein/protein interactions. Libraries of these peptide mimetics with four sites of diversity were prepared according to our previously published solid phase synthetic protocol as shown in Fig. (**2**) [16]. Nucleophilic displacement of the bromide, **1**, with a number of primary amines gave the corresponding secondary amine, **2**, which was then coupled to the appropriate Fmoc-β-amino acids with HOAT/DIC in NMP. Treatment of **3** with 25% piperidine in DMF followed by coupling with Fmoc-β-alanine afforded **4** . After deprotection of the Fmoc group of **4** with 25% piperidine, the resin was treated with the corresponding alkylchloroformate in the presence of DIEA to produce **5**. Cleavage from the acetal resin followed by stereoselective tandem acyliminium cyclization was accomplished by treatment with formic acid at room temperature to give the 6,6-bicyclic mimetic, **6**.

With this synthetic scheme, diversity at the i position of the mimetic is limited to commercially available alkylchloroformates or required the solution phase preparation of the alkyl *p*-nitrophenyl carbonates. Therefore, we have developed an efficient method to furnish diversity at the i position of our template compatible with automated solid-phase synthesis as shown in Fig. (**3**). The Key modifications are utilization of a urea group for stereoselective tandem cyclization to produce the 1,6,8-substituted tetrahydro-2H-pyrazino[1,2-a] pyrimidine-4,7-dione **8** and the on-resin generation of the *p*-nitrophenyl carbamate species **7** that can be derivatized to the corresponding urea **8** by treatment with a variety of amines followed by acid mediated tandem cyclization (Fig. (**3**)) [17].

HPLC analysis of the crude products with monitor-ing at 214 showed the bicyclic mimetics as the major product in all cases. Fig. (**4**) compares the crude NMR spectra with that of the purified product at -20 ˚C. The only impurities observed in this case were polyethyleneglycol and formic acid residue.

Diversity elements were incorporated into the scaffold at the i to i + 3 positions. Four alkoxy groups and sixteen primary amines at the i position, three α-substituted β-alanines at the i + 1 position, fourteen α-amino acids at the i + 2 position, and sixteen primary amines at the i + 3 position were selected for the construction of the library (Fig. (**5**)).

The inhibitory activity of each individual member of the library at 10 μM was evaluated using the TOPFLASH reporter gene assay [19] in SW480 colon carcinoma cells. From the initial screen, we discovered ICG-001 (Fig. (**6**)), which had an IC_{50} of 3 μM (Fig. (**7**)) and good selectivity versus a number of other CBP-dependent reporters including AP-1 (IC_{50} > 100 μM), CRE (IC_{50} > 100 μM), and NFAT (IC_{50} > 50 μM).

DNA microarray analysis using the Clontech Atlas Human Cancer 1.2 Array showed that ICG-001 up-regulated about 2% of the genes more than 2 fold and down-regulated about 0.3% of the genes by greater than 50%. Among the down-regulated genes were two genes, *S100A4* and *survivin*, the number one and four mRNAs unregulated in cancer cells, respectively [20].

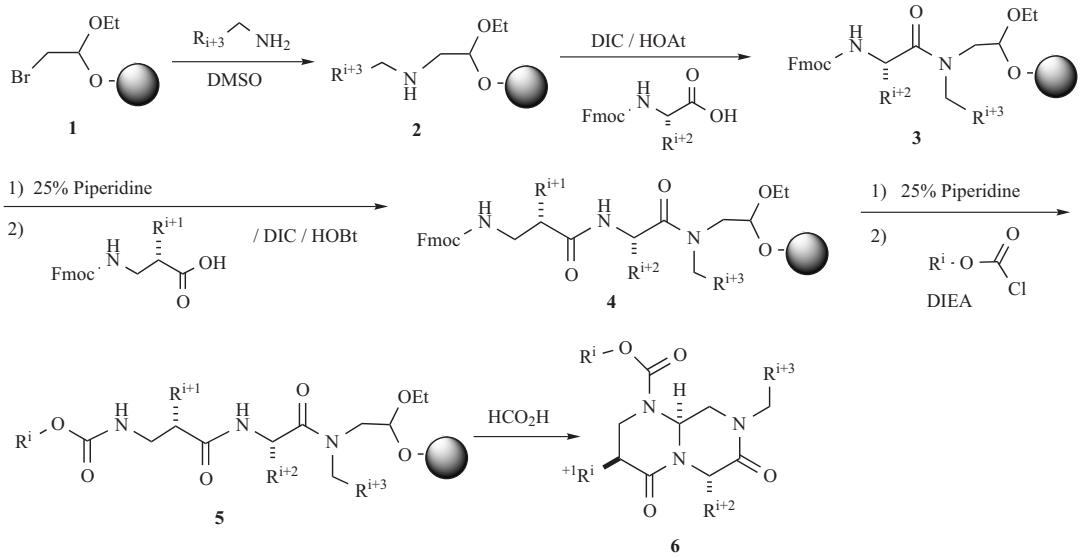

Fig. (2). Synthetic scheme of bicyclic β-turn mimetics **6**.

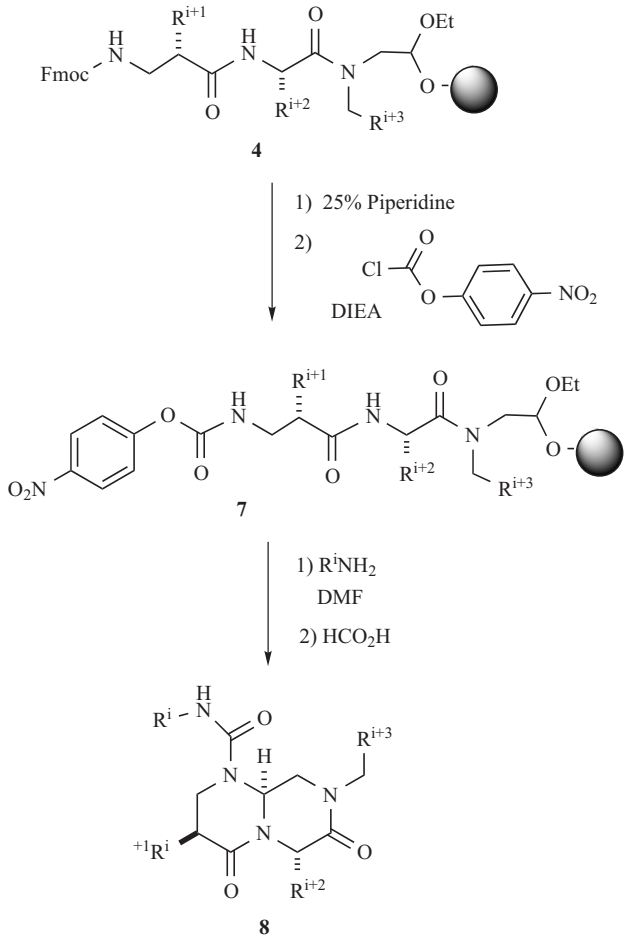

Fig. (3). Synthetic scheme of bicyclic β-turn mimetics **8**.

In order to be considered a lead compound for therapeutic development for colorectal cancer, ICG-001 should demonstrate selective cytotoxicity in colon carcinoma cells. We tested the cytotoxicity of ICG-001 in tumorigenic SW480, HCT116 and normal colonocytes CCD-841Co cells. The results of these studies demonstrate the selective cytotoxicity of ICG-001 at 5 μM in colorectal cancer cells (Fig. (**8**)) [21].

Secondary structure mimetics of proteins are powerful chemogenomic tools for the discovery of small molecule regulators of protein-protein interactions involved in signal transduction and transcriptional regulation. We report the synthesis, discovery and preliminary characterization of ICG-001, a small molecule specific regulator of TCF/β-catenin trascription, from a templated library of diversely functionalized privileged secondary structure mimetics. Further development of ICG-001 is in progress.

EXPERIMENTAL

Fmoc-β-Xaa-α-Xaa-alkylamide-Resin (4)

Bromoacetal resin [Advanced ChemTech or ref. [16]] (1.0 g, 1.0 - 1.4 mmol/g) and a solution of a primary amine in DMSO (10 ml, 2 M) were placed in 20 ml vial with screw cap. The reaction mixture was shaken at 60 ºC using a rotating oven [Robbins Scientific] for 10 – 24 h. The resin was collected by filtration, and washed with DMF, finally DCM. For storage, the resin was dried *in vacuo* at room temperature. A solution of the Fmoc-α-amino acid (3 eq.), HATU (3 eq.), and DIEA (6 eq.) in NMP was added to the resin. After the reaction mixture was shaken for 4 h at room temperature, the resin was filtered and washed with DMF, and then DCM. The loading of the resin was determined at this stage by photometric calibration of the Fmoc chromophore released upon treatment with piperidine. To the resin was added 25% piperidine in DMF (1.5 ml for 100 mg of the resin). After the reaction mixture was shaken for 8 min at room temperature, the resin was filtered and washed with DMF, DCM, and finally DMF. A solution of Fmoc-β-amino acid (3 eq.), HOBT (3 eq.), and DIC (3 eq.) in DMF was added to the resin prepared above. After the reaction mixture was shaken for 3 h at room temperature, the resin was filtered and washed with DMF, DCM, and finally DMF.

(3*S*,6*S*)-Benzyl 8-pentanyl-3,6-dibenzyl-4,7-dioxohexahydro-2H-pyrazino[1,2-a]pyrimidine-1-carboxylate

To the resin (**4**) was added 25% piperidine in DMF (1.5 ml for 100 mg of the resin). After the reaction mixture was shaken for 8 min at room temperature, the resin was filtered and washed with DMF, and then DCM. A mixture of alkylchloroformate (3 eq.) and DIEA (3 eq.) in DCM was added to the resin, the reaction mixture was shaken for 3 h at room temperature. The resin was filtered and washed with DMF, DCM and finally MeOH. The resin was dried *in vacuo* at room temperature. The resin was treated with formic acid (2 ml for 100 mg of resin) for 10 h at room temperature. After the resin was removed by filtration, the filtrate was condensed under reduced pressure to give the crude product.

6a

^{1}H NMR ($CDCl_3$, 500 MHz, -20°C): 0.89 (t, J = 7 Hz, 3H), 1.19 (m, 2H), 1.30 (m, 2H), 1.47 (m, 2H), 2.49 (m, 0.45H), 2.51 (m, 0.45H), 2.57 (dd, J = 9.5, 13.5 Hz, 0.55H), 2.69 (m, 0.55H), 2.75 (q, J = 13 Hz, 0.55H), 2.88 (m, 0.45H), 2.89 (dd, J = 3, 11.5 Hz, 0.55H), 3.05 (m, 0.55H), 3.08 (dd, J = 4, 11.5 Hz, 0.45H), 3.26 (dd, J = 5, 14 Hz, 0.55H), 3.31 (m, 0.55H), 3.33 (m, 0.45H), 3.35 (m, 0.9H), 3.36 (m, 0.9H), 3.42 (d, J = 11 Hz, 0.45H), 3.49 (m, 0.55H), 3.52 (m, 0.55H), 3.59 (m, 0.55H), 3.93 (dd, J = 5.5, 14.5 Hz, 0.45H), 4.04 (dd, J = 5.5, 13 Hz, 0.55H), 4.59 (dd, J = 3, 10 Hz, 0.55H), 4.76 (d, 12.5 Hz, 0.55H), 4.95 (d, 12.5 Hz, 0.45H), 5.11 (d, 12.5 Hz, 0.55H), 5.17 (d, 12.5 Hz, 0.45H), 5.22 (dd, J = 4, 10.5 Hz, 0.45H), 5.24 (t, J = 5 Hz, 0.55H), 5.32 (t, J = 6 Hz, 0.45H), 7.10-7.35 (m, 15H). ESI-MS (pos.); m/z, 554.5 $(M+H)^+$.

(6*S*)-N-Benzyl-6-(*p*-hydroxyphenylmethyl)-8-(1-naphthylmethyl)-4,7-dioxohexahydro-2H-pyrazino[1,2-a]pyrimidine-1-carboxamide

To the resin (**4**) was added 25% piperidine in DMF (1.5 ml for 100 mg of the resin). After the reaction mixture was shaken for 8 min at room temperature, the resin was filtered and washed with DMF, and then DCM. *p*-Nitrophenyl chloroformate (5 eq.) was placed in round-bottomed flask and dissolved in THF. To the solution was

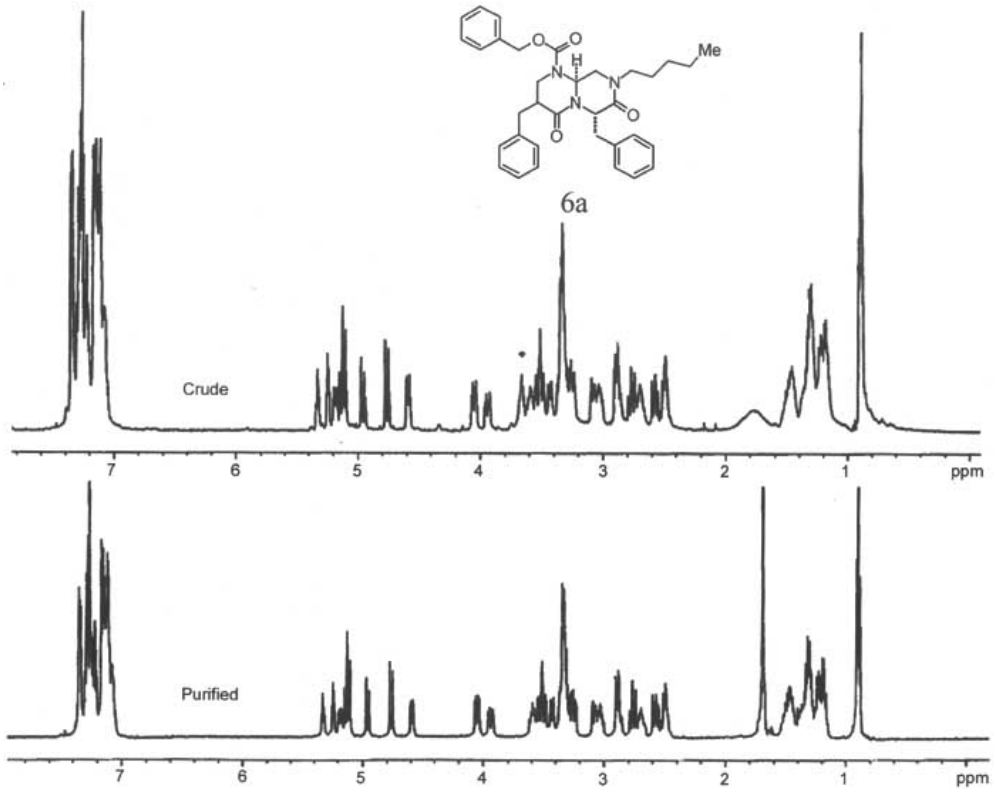

Fig. (4). NMR spectra of crude and purified **6a**.

R^i Position

MeO- EtO - IBuO- BnO-

R^i or R^{i+3} Position

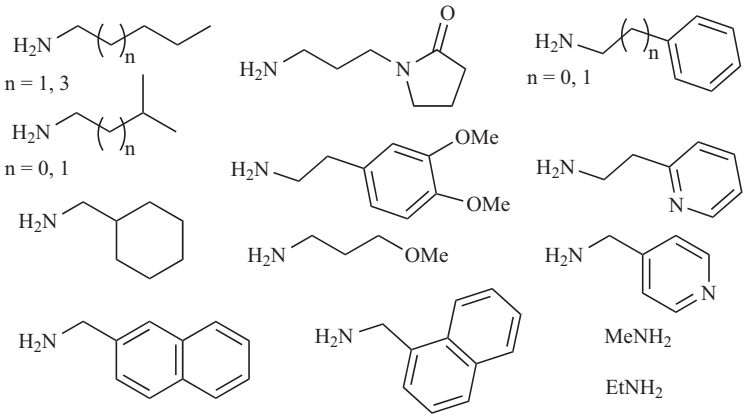

R^{i+1} Position

H, Me, Bn

R^{i+2} Position

Fmoc-Phe	Fmoc-Gly	Fmoc-hPhe	Fmoc-Lys(Boc)
Fmoc-Leu	Fmoc-Ala	Fmoc-Tyr(OBu^t)	Fmoc-Orn(Boc)
Fmoc-Ile	Fmoc-Val	Fmoc-Asp(OBu^t)	
Fmoc-Phg	Fmoc-Met	Fmoc-Glu(OBu^t)	

Fig. (5). Diversity components for the library **Fig. (5)**. Diversity components for the library of bicyclic β-turn mimetics. of bicyclic β-turn mimetics.

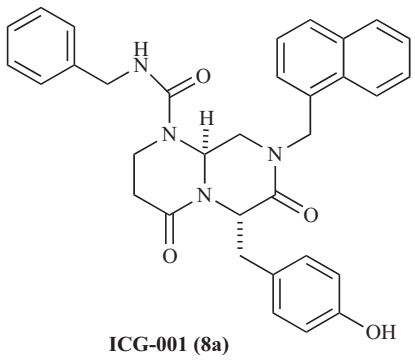

ICG-001 (8a)

Fig. (6). Structure of ICG-001.

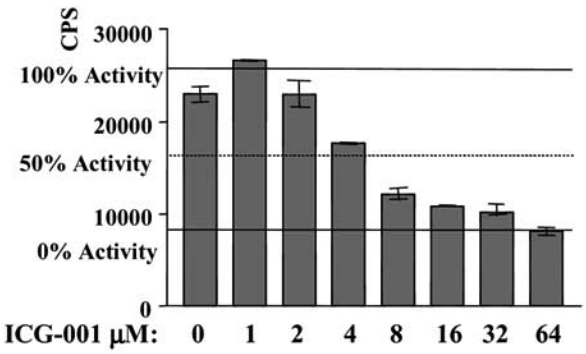

Fig. (7). ICG-001 selectively inhibits the β-catenin/TCF reporter gene construct TOPFLASH. SW480 cells were transfected with TOPFLASH (1.0 µg) treated with ICG-001 (1.0 - 64 µM). Cell lysates were subjected to DUAL-Luciferase Assay 24h post treatment. Values are expressed as mean ± standard deviation.

added DIEA (5 eq) at -20°C and the reaction mixture was slowly warmed to room temperature. The reaction mixture was added to the resin, and shaken for 3 h at room temperature. The resin was filtered and washed with DCM. A solution of amine (4-10 eq) in DMF or DMSO was added to the resin and shaken for 3 h at room temperature followed by filtration and washes with DMF and MeOH. The resin was dried *in vacuo* at room temperature. The resin was treated with formic acid (2 ml for 100 mg of resin) for 10 h at room temperature. After the resin was removed by filtration, the filtrate was condensed under reduced pressure to provide the crude product.

8a

^{1}H NMR ($CDCl_3$, 400 MHz): δ 2.24 (1H, br.d, J = 14 Hz), 2.38 (1H, m), 3.00 (2H, m), 3.16 (1H, t, J = 13 Hz), 3.28 (1H, dd, J = 13 and 5 Hz), 3.41 (1H, dd, J = 13 and 5 Hz), 3.81 (1H, dd, J = 13 and 5 Hz), 4.22 (3H, m), 4.98 (1H, dd, J = 12 and 3 Hz), 5.02 (1H, d, J = 14 Hz), 5.19 (1H, d, J = 14 Hz), 5.40 (1H, t, J = 5 Hz), 6.52 (2H, d, J = 12 Hz), 7.04 (2H, d, J = 12 Hz), 7.10-8.09 (12H, m). ESI-MS (pos.); m/z, 549.0 $(M+H)^+$.

Plasmids

The optimized TOPFLASH and FOPFLASH reporter plasmids [19], β-catenin and Wnt1 expression vectors were provided by Dr. Randall T. Moon (University of Washington). The pRL-null plasmid (Promega), PathDetect pAP1-Luc and pCRE-Luc cis-reporting plasmids (Stratagene) are comercially available.

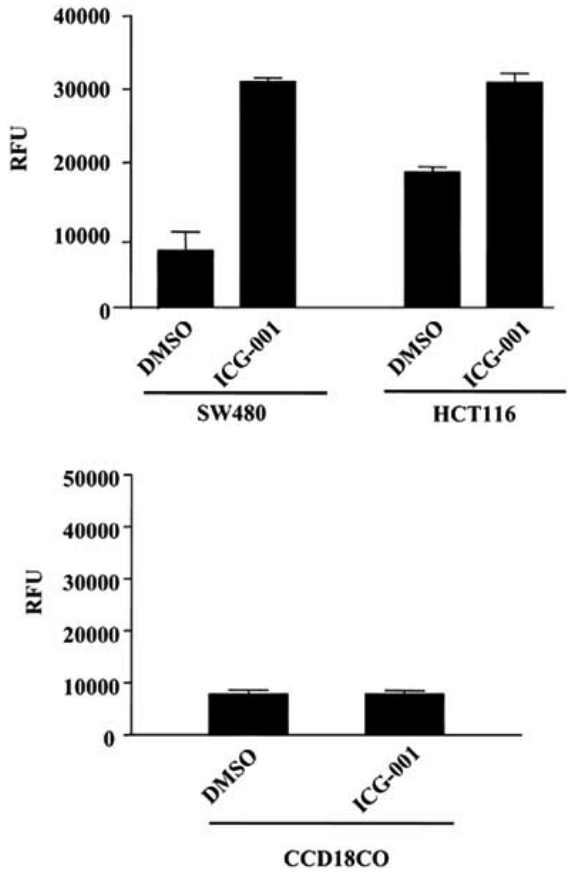

Fig. (8). ICG-001 is selectively cytotoxic to colon carcinoma cell lines, and effective *in vivo*. SW480 and HCT116 cells along with the normal colonic epithelial cells CCD-841Co were treated with ICG-001 (25 µM) or DMSO. Error bars represent mean ± s.d. *, $P < 0.05$.

Cell Culture

The human colon carcinoma cell lines SW480, and HCT116 along with normal colonic epithelial cell line CCD-841Co were all purchased from ATCC, and maintained according to the supplier's recommendations.

Transfection and Luciferase Assays

Cells were transfected using Fugene6 (Roche) with the specified amounts of DNA. We normalized transfection efficiencies using the pRL-null luciferase plasmid. Luciferase assays were performed using the DUAL-Luciferase Reporter Assay System (Promega) according to manufacturer's instructions. All experiments were performed in duplicates. All data represent mean of two independent experiments.

REFERENCES

[1] Moon, R. T.; Bowerman, B.; Boutros, M.; Perrimon, N. *Science* **2002**, *296*, 1644-6.

[2] Morin, P. J. *Bioessays* **1999**, *21*, 1021-30.
[3] Oving, I. M.; Clevers, H. C. *Eur. J. Clin. Invest.* **2002**, *32*, 448-57.
[4] Wodarz, A.; Nusse, R. *Annu. Rev. Cell Dev. Biol.* **1998**, *14*, 59-88.
[5] Gottardi, C. J.; Gumbiner, B. M. *Curr. Biol.* **2001**, *11*, R792-4.
[6] Behrens, J. *Ann N Y Acad. Sci.* **2000**, *910*, 21-33.
[7] Brantjes, H.; Barker, N.; van Es, J.; Clevers, H. *Biol. Chem.* **2002**, *383*, 255-61.
[8] Takemaru, K. I.; Moon, R. T. *J. Cell Biol.* **2000**, *149*, 249-54.
[9] Hecht, A.; Vleminckx, K.; Stemmler, M. P.; van Roy, F.; Kemler, R. *EMBO J* **2000**, *19*, 1839-50.
[10] Moon, R. T.; Kohn, A. D.; De Ferrari, G. V.; Kaykas, A. *Nat. Rev. Genet.* **2004**, *5*, 691-701.
[11] Fearnhead, N. S.; Wilding, J. L.; Bodmer, W. F. *Br. Med. Bull.* **2002**, *64*, 27-43.
[12] Tetsu, O.; McCormick, F. *Nature* **1999**, *398*, 422-6.
[13] Shtutman, M.; Zhurinsky, J.; Simcha, I.; Albanese, C.; D. Amico, M.; Pestell, R.; Ben-Ze ev, A. *Proc. Natl. Acad. Sci. USA* **1999**, *96*, 5522-7.
[14] He, T. C.; Sparks, A. B.; Rago, C.; Hermeking, H.; Zawel, L.; da Costa, L. T.; Morin, P. J.; Vogelstein, B.; Kinzler, K. W. *Science* **1998**, *281*, 1509-12.

Received: 02 June, 2005 Accepted: 03 June, 2005

[15] Kim, J. S.; Crooks, H.; Foxworth, A.; Waldman, T. *Mol. Cancer Ther.* **2002**, *1*, 1355-9.
[16] Eguchi, M.; Lee, M. S.; Nakanishi, H.; Stasiak, M.; Lovell, S.; Kahn, M. *: J. Am. Chem. Soc.* **1999**, *121*, 12204-12205.
[17] Eguchi, M.; Lee, M. S.; Stasiak, M.; Kahn, M. *Tetrahedron Lett.* **2001**, *42*, 1237-1239.
[18] Wilmot, C. M.; Thornton, J. M. *J. Mol. Biol.* **1988**, *203*, 221-232.
[19] Korinek, V.; Barker, N.; Morin, P. J.; van Wichen, D.; de Weger, R.; Kinzler, K. W.; Vogelstein, B.; Clevers, H. *Science* **1997**, *275*, 1784-7.
[20] Velculescu, V. E.; Madden, S. L.; Zhang, L.; Lash, A. E.; Yu, J.; Rago, C.; Lal, A.; Wang, C. J.; Beaudry, G. A.; Ciriello, K. M.; Cook, B. P.; Dufault , M. R.; Ferguson, A. T.; Gao, Y.; He, T. C.; Hermeking, H.; Hiraldo, S. K.; Hwang, P. M.; Lopez, M. A.; Luderer, H. F.; Mathews, B.; Petroziello, J. M.; Polyak, K.; Zawel, L.; Kinzler, K. W. *Nat. Genet.* **1999**, *23*, 387-8.
[21] Emami, K. H.; Nguyen, C.; Ma, H.; Kim, D. H.; Jeong, K. W.; Eguchi, M.; Moon, R. T.; Teo, J. L.; Oh, S. W.; Kim, H. Y.; Moon, S. H.; Ha, J. R.; Kahn, M. *Proc. Natl. Acad. Sci. USA* **2004**, *101*, 12682-7.